

Pediatric Cardiac-Gated CT Angiography: Assessment of Radiation Dose

Caroline L. Hollingsworth¹
 Terry T. Yoshizumi^{1,2}
 Donald P. Frush¹
 Frandics P. Chan³
 Greta Toncheva²
 Giao Nguyen²
 Carolyn R. Lowry¹
 Lynne M. Hurwitz¹

Keywords: CT angiography, dosimetry, pediatric radiology, radiation dose

DOI:10.2214/AJR.06.1507

Received November 13, 2006; accepted after revision February 19, 2007.

¹Department of Radiology, Division of Pediatric Radiology, 1905 McGovern-Davison Children's Health Center, Box 3803, Department of Radiology, Duke University Medical Center, Durham, NC 27710. Address correspondence to C. L. Hollingsworth (holl016@mc.duke.edu).

²Division of Radiation Safety, Duke University Medical Center, Durham, NC.

³Department of Radiology, Stanford University Medical Center, Palo Alto, CA.

AJR 2007; 189:12–18

0361–803X/07/1891–12

© American Roentgen Ray Society

OBJECTIVE. The purpose of our study was to determine a dose range for cardiac-gated CT angiography (CTA) in children.

MATERIALS AND METHODS. ECG-gated cardiac CTA simulating scanning of the heart was performed on an anthropomorphic phantom of a 5-year-old child on a 16-MDCT scanner using variable parameters (small field of view; 16 × 0.625 mm configuration; 0.5-second gantry cycle time; 0.275 pitch; 120 kVp at 110, 220, and 330 mA; and 80 kVp at 385 mA). Metal oxide semiconductor field effect transistor (MOSFET) technology measured 20 organ doses. Effective dose calculated using the dose-length product (DLP) was compared with effective dose determined from measured absorbed organ doses.

RESULTS. Highest organ doses included breast (3.5–12.6 cGy), lung (3.3–12.1 cGy), and bone marrow (1.7–7.6 cGy). The 80 kVp/385 mA examination produced lower radiation doses to all organs than the 120 kVp/220 mA examination. MOSFET effective doses (± SD) were as follows: 110 mA: 7.4 mSv (± 0.6 mSv), 220 mA: 17.2 mSv (± 0.3 mSv), 330 mA: 25.7 mSv (± 0.3 mSv), 80 kVp/385 mA: 10.6 mSv (± 0.2 mSv). DLP effective doses for diagnostic runs were as follows: 110 mA: 8.7 mSv, 220 mA: 19 mSv, 330 mA: 28 mSv, 80 kVp/385 mA: 12 mSv. DLP effective doses exceeded MOSFET effective doses by 9.7–17.2%.

CONCLUSION. Radiation doses for a 5-year-old during cardiac-gated CTA vary greatly depending on parameters. Organ doses can be high; the effective dose may reach 28.4 mSv. Further work, including determination of size-appropriate mA and image quality, is important before routine use of this technique in children.

Catheter-directed cardiac angiography is the recognized gold standard for assessment of coronary artery anatomy and complex cardiovascular anomalies in children, but it has the potential to impart high radiation doses because of extended fluoroscopic and cine evaluation [1–3]. Additional relative disadvantages of cardiac angiography include procedure-related complications (pseudoaneurysm, vessel dissection, stroke) and expense related to resources needed, including specialized equipment and personnel. These factors have led to the investigation of alternative techniques for diagnostic evaluation of the cardiovascular system [4, 5]. Technical advances for less resource-demanding and less invasive procedures, including MDCT angiography (CTA), have resulted in a rapid increase in use of this technique for cardiac evaluation. These technical advances include faster gantry rotation cycle times (≤ 500 milliseconds) narrower (submillimeter) detector

widths, and increasing numbers (e.g., 64) of detector rows combining to improve image quality by increasing spatial resolution and decreasing motion artifacts. In addition, image degradation from cardiac motion is further reduced using retrospective ECG gating or prospective ECG triggering [6–8].

Cardiac-gated CTA is being used in the assessment of coronary arteries in adults [9–12]. However, imaging the heart and coronary arteries using cardiac-gated CTA has not been systematically assessed in children. Systematic assessment includes determination of the parameters that contribute to radiation dose from cardiac-gated CTA. For example, optimal tube current and kilovoltage settings are still evolving in adults even as the number of cardiac-gated CTA examinations is increasing [13]. In addition, attention has recently been directed to dosimetry of cardiac-gated CTA [14–23]. However, one difficulty in assessing CT dose is that traditional methodology using thermoluminescent dosimeters (TLDs) is prob-

Pediatric Cardiac-Gated CT Angiography

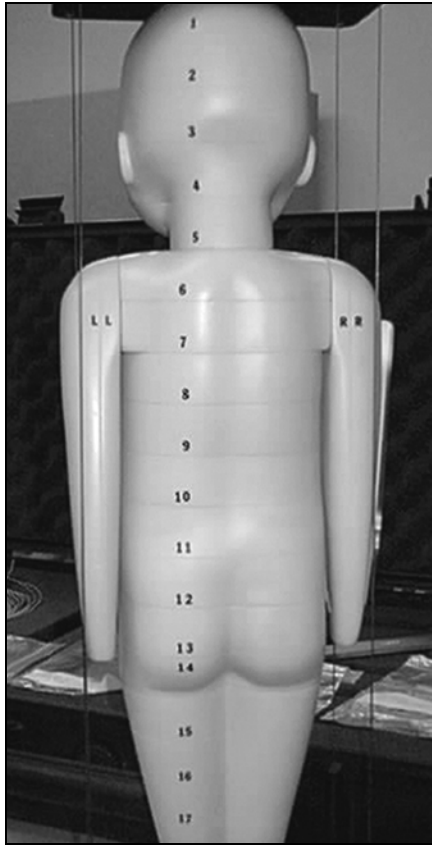


Fig. 1—Posterior view of anthropomorphic phantom of 5-year-old child depicts axial slices that contain tissue-equivalent anatomic sites labeled 1–17, LL = left and RR = right.

lematic, especially for assessing multiple CT examinations because multiple phantoms or repeated loading of dosimeters into a single phantom is necessary. An alternative method of dose assessment using the dose-length product (DLP) has been studied but has recently been challenged as imprecise [24, 25]. A relatively new combination of dosimetry using metal oxide semiconductor field effect transistor (MOSFET) technology and adult and pediatric anthropomorphic phantoms has overcome many of these technical dosimetry difficulties [26–35]. To our knowledge, to date this combination has not been applied to pediatric cardiac-gated CTA radiation dose assessment.

It is essential to balance image quality and radiation dose delivered when performing CTA in children [36, 37] including cardiac-gated CTA. Part of this balance is knowing how much radiation dose is delivered. Therefore, the specific purpose of this investigation was to measure the radiation dose resulting from a range of techniques for cardiac-gated CTA in a pediatric anthropomorphic phantom.

TABLE 1: Specific Organ Radiation Dose (cGy) Measured by MOSFET During Cardiac-Gated CT Angiography in Anthropomorphic Phantom of 5-Year-Old Child

Organ Location	Protocol ^a				Timing Bolus
	110 mA/120 kVp	220 mA/120 kVp	330 mA/120 kVp	385 mA/80 kVp	
BM, mandible	0	0	0	0	0
Thyroid	0.2 (± 0.3)	0.7 (± 0.3)	0.7 (± 0.1)	0.2 (± 0.2)	0
Esophagus	0.5 (± 0.1)	1.2 (± 0.1)	1.9 (± 0.1)	0.6 (± 0.0)	0.1 (± 0.0)
BM, rib	0.9 (± 0.2)	2.1 (± 0.3)	3.2 (± 0.2)	1.1 (± 0.3)	0.2 (± 0.0)
Lungs (top)	3.5 (± 0.1)	7.4 (± 0.4)	11.3 (± 0.3)	4.3 (± 0.2)	2.7 (± 0.0)
Breast, left	3.5 (± 0.3)	8.4 (± 0.4)	12.6 (± 0.4)	5.9 (± 0.1)	4.6 (± 0.1)
Breast, right	3.3 (± 0.2)	7.3 (± 0.4)	11.4 (± 0.4)	4.7 (± 0.2)	3.0 (± 0.0)
Lungs (middle)	3.7 (± 0.3)	8.2 (± 0.4)	12.1 (± 0.2)	5.2 (± 0.2)	0.2 (± 0.0)
Lungs (low)	3.3 (± 0.2)	6.9 (± 0.8)	11.0 (± 0.7)	4.3 (± 0.3)	0.1 (± 0.0)
BM, thoracic spine	1.7 (± 0.1)	4.1 (± 0.1)	6.7 (± 0.2)	1.9 (± 0.2)	0
Liver	0.7 (± 0.1)	1.5 (± 0.2)	2.5 (± 0.1)	0.8 (± 0.0)	0
Stomach	0.2 (± 0.1)	0.6 (± 0.2)	0.9 (± 0.1)	0.2 (± 0.0)	0
Kidney	0.3 (± 0.2)	0.5 (± 0.1)	1.0 (± 0.1)	0.2 (± 0.1)	0
Intestine	0	0.4 (± 0.1)	0.6 (± 0.0)	0.2 (± 0.1)	0
Ascending colon	0	0	0.2 (± 0.1)	0	0
BM, lumbar spine	0	0	0	0	0
BM pelvis	0	0	0	0	0
Ovaries (gonads)	0	0	0	0	0
Bladder	0	0	0	0	0
Testes	0	0	0	0	0

Note—Data are doses in cGy. MOSFET = metal oxide semiconductor field effect transistor, BM = bone marrow.
^aCardiac-gated CTA examinations performed on a 16-MDCT scanner (LightSpeed, GE Healthcare) using SnapShot Burst Plus software.

Materials and Methods

A tissue-equivalent anthropomorphic phantom (Model 705-D, CIRS) of a 5-year-old child was used in this study (Fig. 1). This age was used because the phantom was one of only two available in the department and because dosimetry for a 5-year-old is better applied to older and younger ages than a neonatal phantom. Organ dose measurements were obtained using the MOSFET AutoSense system (Model TN-RD-60, Thomson-Nielsen, a division of Best Medical Canada, Ltd.) that consists of 20 high-sensitivity detectors (Model TN-1002RD, Thomson-Nielsen) connected to four bias supplies. These MOSFET detectors are specifically intended for diagnostic radiology applications.

MOSFET detectors were calibrated as follows. First, we determined the thickness of copper sheets to achieve the half-value layer (HVL) (7.24 mm Al at 120 kVp) of GE Healthcare CT scanners [27] with a conventional radiographic X-ray tube; we added 0.2-mm copper sheets to the X-ray tube to obtain an equivalent HVL of 7.37 mm Al at 120 kVp. After this had been accomplished, individual MOSFET detectors were calibrated at a clinical en-

ergy of 120 kVp. Individual calibration factors were obtained for all 20 MOSFET detectors by fitting four data points with the least-squares fit routine (Prism, version 2.0, 1995, GraphPad software). These conversion factors were stored in the MOSFET software (AutoSense PC software version 2–1, TN-RD-49, Thomson-Nielsen) for immediate readout after each protocol was performed. The bias supplies provide a regulated bias voltage to the detectors and are connected to a reader after a radiation exposure to measure the threshold voltage shift in the detector. This permanent shift in the threshold voltage after irradiation is proportional to the absorbed radiation dose [38].

The MOSFET sensors gathered data from 20 simulated anatomic sites in the tissue-equivalent phantom (Table 1). The leads were placed to measure doses at specific organ locations in the phantom, which was configured of individual slices containing anthropomorphic tissue equivalents (Fig. 1). The data were directly sent to a laptop computer after each exposure. Subsequently, the effective radiation dose was calculated according to guidelines published in International Commission on Radiological

TABLE 2: Scanning Parameters and Console Radiation Dosimetry for SnapShot Burst Plus 0.625-mm Protocol in Anthropomorphic Phantom of 5-Year-Old Child

Parameter	kVp	mA	Pitch ^a	Time for Complete Tube Rotation (s)	Exposure Time (s)	SFOV	CTD _{1vol} (mGy)	DLP (mGy · cm)
Low mA	120	110	0.625 mm 2.75 0.275:1	0.5	17.8	Small	41.97	411.88
Medium mA	120	220	0.625 mm 2.75 0.275:1	0.5	17.8	Small	91.31	896.01
High mA	120	330	0.625 mm 2.75 0.275:1	0.5	17.8	Small	136.97	1,344.02
Low kVp	80	385	0.625 mm 2.75 0.275:1	0.5	17.8	Small	57.53	564.49
Timing bolus	120	400	0.625 mm 2.75 0.275:1	0.8	9.6	Small	544.35	1,088.69

Note—Cardiac-gated CTA examinations were performed on 16-MDCT scanner (LightSpeed, GE Healthcare) using SnapShot Burst Plus software (GE Healthcare). SFOV = scanning field of view, CTD_{1vol} = volume CT dose index, DLP = dose-length product.

^aFirst value is slice thickness, second value is reconstruction interval, and third value is true pitch.

Protection (ICRP) 60 by summing the products of the average recorded organ radiation dose and the ICRP weighting factor [39]. Radiation doses measured in tissue equivalents for small organs such as the ovary and thyroid gland were through a single-detector scanner only. In comparison, radiation doses measured in larger organs such as the liver or lung were calculated after determination of the mean of several-detector dose measurements. Pediatric bone marrow distributions were previously published by Cristy [40]. We have used percentage of bone marrow distribution data for 5-year-olds in the effective dose calculations for the major skeletal regions: skull (cranium + mandible) (17.44%), ribs (ribs + sternum) (10.58%), spine (middle portion) (9.58%), and pelvis (23.33%).

The effective dose was also calculated by the DLP displayed on the CT console for each protocol. The general formula for effective dose is as follows:

$$\text{Effective dose} = E_{\text{DLP}} \times \text{DLP},$$

where the effective dose is measured in mSv (for this investigation a conversion factor of 0.021 mSv per mGy · cm was used to estimate the effective dose); effective dose_{DLP} is an anatomy-specific dose coefficient expressing effective dose normalized to DLP in mSv · mGy⁻¹ · cm⁻¹, and DLP is in

mGy · cm [41]. A conversion factor of 0.021 was used based on the following: the adult conversion factor for chest CT is 0.017, and conversion factors for young children should be larger than adult conversion factors [41]; there are no published conversion factors for pediatric chest CT; and additional work in our dosimetry laboratory (unpublished data) with the phantom of the 5-year-old child and MOSFET technology for chest MDCT indicates that the conversion factor of 0.021 mSv · mGy⁻¹ · cm⁻¹ is reasonable.

The retrospective gated cardiac CT examinations were performed on a 16-MDCT scanner (LightSpeed, GE Healthcare) using the SnapShot Burst Plus software (GE Healthcare), which creates an image made with 180° rotation. Multisector reconstruction is used to improve temporal resolution to better than 250 milliseconds. The specific scanning parameters are summarized in Table 2. In the absence of published protocols for pediatric cardiac-gated CT angiography, three different protocols were arbitrarily designed to cover a range of potential doses delivered during gated CT angiography. These diagnostic phase protocols consist of modifications of tube current (in milliamperes) arbitrarily designated as high (330 mA), medium (220 mA), and low (110 mA), corresponding to the milliamperage value. ECG dose modulation was not

available, and thus mA was fixed throughout each examination. The peak kilovoltage (kVp) was kept constant at 120 kVp for these tube currents. The high mA protocol was chosen to represent the tube current that is currently in use in clinical practice in adults because conceivably that could be a default protocol for pediatric imaging [42]. We were also interested in assessing dose for a lower kVp protocol because reduced kVp has been advocated in pediatric MDCT, including CTA [35], so an additional protocol using 80 kVp and an mA of 385 was performed. Based on data that a decrease in kVp from 120 to 80 results in an increase in noise of 68% [43], an increased tube current was used to partially compensate for this. The tube current was increased from 220 to 385 mA (75% increase), yielding a predicted decrease in noise of 33%. Because contrast improves with lower kVp, a balance in noise was not attempted. This protocol was not selected to be an equivalent in noise to the 220 mA/120 kVp protocol, but is a representation of a protocol used at one investigator's institution after consultation with the manufacturer of the MDCT scanner. Dosimetry was also performed for the timing bolus exposure at 5-mm axial acquisition, 0.8 second gantry rotation time, 40 mA, and 120 kVp.

The phantom was examined in the supine position with a single diagnostic phase examination from the carina to the cardiac apex (10 cm) using retrospective cardiac gating (Fig. 2). A heart rate simulator (ECG Simulator, model GE Marquette, GE Healthcare) was used, set at a rate of 100 beats per minute representing a normal heart rate for a 5-year-old child [44]. Each of the four diagnostic phase examinations and a single timing bolus phase were performed three consecutive times. The organ doses obtained during each of the three exposures were used to obtain an average dose value and SD for each protocol. During each examination, the same dosimeters were exposed in identical locations to minimize recorded dose bias due to intrinsic measurement disparities. The effective organ doses discussed in this article are therefore the summed averages of the three simulated scans for each protocol. MOSFET effective dose was determined using ICRP 60 guidelines [45, 46] and compared with the DLP effective dose, calculated using methodology by Shrimpton and Wall [41].

Results

The measured radiation doses (and SDs) to specific organs are summarized in Table 1, and select organ doses are depicted in Figure 3. The MOSFET effective doses for the four different protocols are provided in Table 3 and Figure 4.

Organ dose measurements varied depending on the specific protocol evaluated. When

Pediatric Cardiac-Gated CT Angiography

Fig. 2—Anthropomorphic phantom of 5-year-old child positioned supine in CT gantry with metal oxide semiconductor field effect transistor (MOSFET) system and heart rate simulator.



Fig. 3—Organ doses were calculated using summed averages of three simulated scans for each protocol. Effective dose was determined using ICRP 60 (International Commission on Radiological Protection) guidelines [39]. BM = bone marrow.

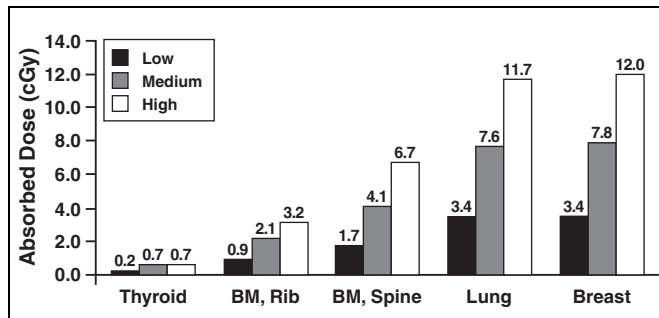


TABLE 3: Effective Dose for Pediatric Cardiac-Gated CT Angiography with SnapShot Burst Plus 0.625 mm Software^a Using ICRP 60 as Reference Standard

Scanning Parameters	Effective Dose (mSv)	Effective Dose + Timing Bolus (mSv)
330 mA, 120 kVp	25.7 + 0.3	28.4 + 0.3
220 mA, 120 kVp	17.2 + 0.3	19.9 + 0.3
110 mA, 120 kVp	7.4 + 0.6	10.1 + 0.6
385 mA, 80 kVp	10.6 + 0.2	13.3 + 0.2
Timing bolus	2.7 + 0.1	—

Note—Total effective dose was calculated using guidelines of International Commission on Radiological Protection (ICRP) [39]. Dash (—) indicates not applicable.

^aGE Healthcare.

assessing the doses calculated for the three protocols with constant kVp (120 kVp), the low-mA (110 mA) protocol imparted a lower

radiation dose to all organs than the medium-mA (220 mA) or the high-mA (330 mA) protocols, as expected. However, this investigation provided an opportunity to assess organ doses (Table 1). We found that the highest organ dose from all protocols was to the lungs and the breast. The combined breast dose was 3.4 cGy (right and left breasts averaged) for the low-mA (110 mA, 120 kVp) protocol, 8.0 cGy for the medium-mA (220 mA, 120 kVp) protocol, and 12 cGy for the high-mA (330 mA, 120 kVp) protocol. The lung dose (top, middle, and lower lung lobe doses averaged) was 3.5 cGy for the low-mA (110 mA, 120 kVp) protocol, 7.5 cGy for the medium-mA (220 mA, 120 kVp) protocol, and 11.6 cGy for the high-mA (330 mA, 120 kVp) protocol. The 385 mA/80 kVp protocol delivered 5.3 cGy as a breast dose and 4.6 cGy as a lung dose, which are lower doses than either the medium-mA or high-mA protocols.

The MOSFET effective doses for the four different protocols are provided in Table 3

and Figure 4. These results show the expected reduction in the resultant effective dose as the mA is reduced by one third for the medium- and by two thirds for the low-dose protocols, as compared with the high-mA protocol. That is, our results show the predicted drop in effective dose from 28.4 to 19.9 mSv (measured, 30%; expected, 33.3%) and finally to 10.1 mSv (measured, 64%; expected, 66.7%) as the tube current changed from 330 to 220 mA and finally to 110 mA.

The effective dose for the 80-kVp examination, including the timing bolus, was 13.3 ± 0.2 mSv. The low-kVp examination as designed (385 mA, 80 kVp) had a lower effective dose than the CT protocols with medium mA (220 mA, 120 kVp) and high mA (330 mA, 120 kVp). For diagnostic scanning, the effective dose calculated from the DLP method was always higher than the measured effective dose, and differed from between 9.7% to 17.2% (Fig. 5).

Discussion

Although technologic innovation often heralds new or improved diagnostic benefits, it is prudent to approach these benefits with an understanding of additional costs and risks, and for CT this includes the radiation dose. As CTA and gated-cardiac CTA become increasingly used for the evaluation of the cardiovascular system in the pediatric population [47, 48], knowledge and understanding of the radiation dose are imperative. This is in part due to both increased radiosensitivity in the pediatric population and the longer lifetime for radiation-induced stochastic effects to manifest in children [24, 34, 46, 49–53].

Therefore, establishing MDCT radiation doses is a necessity for both clinical management of patients and for institutional review board risk assessment for research. However, establishing these doses has been problematic. The traditional method for quantification of radiation dose using thermoluminescent dosimeters (TLDs) is time-consuming. For example, loading, unloading, and processing the TLDs must follow each CT examination. Therefore, only one CT examination can be performed at a time (unless another phantom with TLDs is available), and dosimeters may have to be shipped to another site for interpretation. The MOSFET technique for dosimetry provides real-time dosimetry in which data from multiple CT examinations can be acquired instantaneously during a single session. MOSFET dosimetry is particularly useful in the comparison of doses from multiple

Fig. 4—Total effective dose was determined using ICRP 60 (International Commission on Radiological Protection) guidelines [39] and using doses from average of three scans for each protocol and timing bolus.

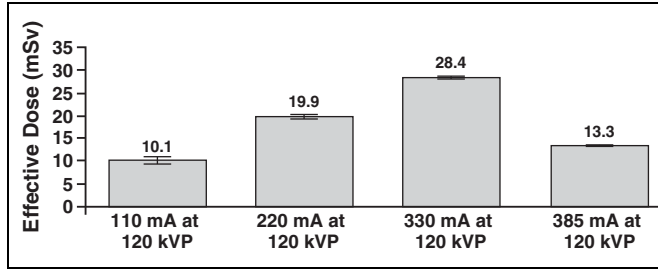
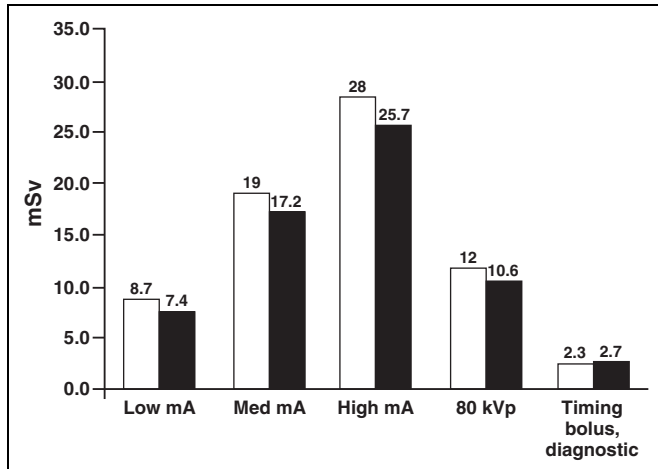


Fig. 5—Effective dose calculated from dose-length product (DLP) (*white*) on CT console was compared with effective dose calculated from ICRP 60 (International Commission on Radiological Protection) guidelines (*black*) for four diagnostic protocols. In all instances, effective dose calculated from DLP was 9.7% to 17.2% higher. Note that only effective doses for diagnostic runs are depicted in graph.



CT protocols in which the dose effect of various manipulations such as alteration of mA, kVp, or pitch can be assessed. MOSFET technology has previously been validated against the TLD method; it also provides an accurate method to assess dose, with uncertainty in dose recorded during the three separate runs for each protocol in the range of 10% at the 1-cGy dose level [25, 34].

Based on this MOSFET dosimetry, cardiac-gated CTA doses to a 5-year-old can exceed 28 mSv when a protocol with adult techniques is used. These doses are well beyond those used for routine chest CT in adults (5.4 mSv) or children (< 5 mSv) [25, 54, 55]. For the child, the dose is up to 5.6 times the radiation dose of routine chest CT. For diagnostic scanning, the effective dose calculated using the DLP method was consistently higher (9.7–17.2%) than the effective dose calculated from the ICRP 60 guidelines [39]. The DLP is available on most modern CT scanners, and our data show that although overestimation occurs consistently, the DLP method provides a reasonable estimate, we believe, for the effective dose for cardiac-gated CTA in a 5-year-old. This difference, however, may not be reflected at different ages (cross-sectional areas) or when using a different field

of view, and it obviously depends on the conversion factor used.

Our dosimetry data also provide an opportunity to compare radiation doses from cardiac-gated CTA with those from conventional angiography. The radiation dose delivered to the 5 year-old using an adult protocol also exceeds the dose reported for adults. Several recent investigations of the radiation dose delivered by coronary cardiac-gated CTA in adults have found the potential radiation dose to be relatively high (up to 18.8 mSv) depending on the type of scanner [21, 23, 56]. Using results from Hunold et al. [13], our data also indicate that the dose delivered by cardiac-gated CTA may be as great as 2.5 times the dose delivered by conventional angiography. Bacher et al. [57] report median effective doses of 4.6 mSv for diagnostic pediatric cardiac catheterizations and 6.0 mSv for therapeutic cardiac catheterizations. Similar measurements are reported by Rassow et al. [58], who found effective dose measurements from cardiac catheterization in infants to range from 2 mSv (25th percentile) to nearly 18 mSv (90th percentile). In comparison, the preliminary data with our pediatric phantom indicate that there is potential for the radiation dose to children undergoing cardiac-gated CTA to be substantially higher than the

dose delivered by standard cardiac catheterization. If a high-dose technique is used, the dose to a child for cardiac-gated CTA may be up to six times (28 vs 4.6 mSv) that of a standard cardiac catheterization.

As shown in an anthropomorphic phantom of a 5-year-old, cardiac-gated CTA in children can result in a higher radiation dose than conventional angiography. However there are benefits of CT versus conventional catheterization in children. Cardiac catheterization is invasive. Complications associated with femoral artery catheterization include occlusion, dissection, pseudoaneurysm formation, and retroperitoneal hemorrhage [57, 58]. Furthermore, serious sequelae such as limb growth discrepancy can occur because of arterial ischemia in infants and young children [55, 58–61]. Postprocedural monitoring may require several hours in a recovery unit. Cardiac catheterization may also require general anesthesia. Cardiac-gated CTA does not require the same frequency of sedation as conventional angiography and requires only that there be adequate venous access [35, 62]. Although no reports of sedation frequency are available to our knowledge, the limited need for sedation in these examinations would likely also apply because the examination is rapidly acquired and can be performed in seconds. Cardiac-gated CTA can easily be completed using 1.5 mL/kg of IV contrast material, which is less than the amount generally required for cardiac catheter angiography [35]. If the IV access site allows power injection, no ancillary staff is exposed to radiation (e.g., when a manual bolus technique is used, the individual responsible for the injection must be in the room during at least a portion of the image acquisition). The procedure itself imparts a radiation dose to the child and the physician performing the examination, and any support staff who are required to be present in the angiography suite [63–65].

Because CT angiography in children can be performed at a lower kVp, which will increase the inherent tissue contrast [35, 43, 63] and potentially improve the contrast-to-noise ratio, we elected to study a lower-kVp protocol. It was not our intention to maintain image noise compared with the three protocols performed at 120 kVp, but to select a kVp level that has been advocated in the literature for pediatric CTA and to partially compensate for the increased noise with an increase in tube current to 385 mA. With this protocol, the measured dose was less than with the 220 mA/120 kVp protocol but higher than with the lowest mA

protocol. These data indicate that dose levels can be achieved in the lower range when a lower kVp is used, although more work must be done to assess the overall affect on image quality, considering both mottle and contrast.

Our investigation has several limitations. The examination was performed for only one age phantom. We chose a phantom of a 5-year-old because of availability and because this phantom better approximated the range of children evaluated from infancy through early teens. In addition, the examinations were all performed on a single scanner type with select protocols. Although the adult parameters arguably would not be the default, to our knowledge no pediatric cardiac-gated CTA guidelines have been systematically investigated. We chose the specific protocols in this investigation to represent high-, medium-, and low-dose protocols to assess a range of potential doses.

Another limitation is that there was no investigation of image quality or the potential effect of changes in protocol on image quality. Our investigation also did not evaluate the potential benefits (decreased dose) due to dose modulation techniques because our institution did not have this capability during the period of the investigation. It has been reported that this technique can reduce the radiation dose by 30–50% by significantly reducing the tube current during systole [66]. Also, some discrepancies were seen in organ doses measured by MOSFET. We believe the discrepancy in dose to the breast relative to that imparted on the lungs with the low-mA (110 mA) protocol may be explained by the helical rotation of the X-ray tube and the variation of the dose measured when the breast is positioned as a surface organ versus its exposure when the X-ray beam passes through the chest from back to front. The lungs received a more uniform exposure because of their relatively central position in the chest. The changes in relative position of the breast and the X-ray beam source may also explain slight differences in dose received by the right and left breasts. We performed three runs for each protocol to reduce the positional effect of the detectors. Although performing an axial acquisition of data would eliminate this sampling issue based on detector position, this technique is not practical for cardiac-gated evaluation.

Finally, we used an estimated conversion factor of $0.021 \text{ mSv} \cdot \text{mGy}^{-1} \cdot \text{cm}^{-1}$ for pediatric chest MDCT based on justifications in the methodology. In fact, when we computed a dose conversion factor (effective_{DLP}) from MOSFET results, we arrived at a conversion factor of 0.019 using the equation:

$$\text{effective}_{\text{DLP}} = \text{effective dose from measurements of phantom of 5-year-old} / \text{DLP(console display)}.$$

This confirms that our initial estimate of $0.021 \text{ mSv} \cdot \text{mGy}^{-1} \cdot \text{cm}^{-1}$ for effective_{DLP} was reasonable and slightly more conservative than the phantom-based value of $0.019 \text{ mSv} \cdot \text{mGy}^{-1} \cdot \text{cm}^{-1}$.

In conclusion, technical advances in cardiac imaging with cardiac-gated CTA are rapidly evolving. MOSFET technology is a useful tool for measuring radiation dose from cardiac-gated CTA protocols and can provide radiation dose quantification. Depending on parameters, these doses vary substantially and can be relatively high, with the effective dose reaching 28.4 mSv in the protocols tested; some of the highest organ doses are to the pediatric breast. More information is needed for development of optimal scanning parameters and assessment of the diagnostic accuracy of this technique before its widespread use in the pediatric population.

References

- Bakalyar DM, Castellani MD, Safian RD. Radiation exposure to patients undergoing diagnostic and interventional cardiac procedures. *Cathet Cardiovasc Diagn* 1997; 42:121–125
- Van de Putte S, Verhaegen F, Taeymans Y, et al. Correlation of patient skin doses in cardiac interventional radiology with dose area product. *Br J Radiol* 2000; 73:504–513
- Bacher K, Bogaert E, Lapere R, et al. Patient-specific dose and radiation risk estimation in pediatric cardiac catheterization. *Circulation* 2005; 111:83–89
- Kennedy JW. Complications associated with cardiac catheterization and angiography. *Cathet Cardiovasc Diagn* 1982; 8:5–11
- Gersh BJ, Kronmal RA, Frye RL, et al. Coronary arteriography and coronary artery bypass surgery: morbidity and mortality in patients ages 65 years or older—a report from the Coronary Artery Surgery Study. *Circulation* 1983; 67:483–491
- Morgan-Hughes GJ, Roobottom PE, Marshal AJ. Highly accurate coronary angiography with submillimeter, 16 slice computed tomography. *Heart* 2005; 91:308–313
- Flohr T, Kuttner A, Bruder H, et al. Performance evaluation of a multi-slice CT system with 16-slice detector and increased gantry rotation speed for isotropic submillimeter imaging of the heart. *Herz* 2003; 28:7–19
- Manghat NE, Morgan-Hughes GJ, Marshal AJ, Roobottom CA. Multidetector row computed tomography: imaging the coronary arteries. *Clin Radiol* 2005; 60:939–952
- Schroeder S, Kopp AF, Baumbach A, et al. Noninvasive detection of coronary lesions by multislice computed tomography: results of the new age pilot trial. *Catheter Cardiovasc Interv* 2001; 53:352–358
- Achenbach S, Ulzheimer S, Baum U, et al. Noninvasive coronary angiography by retrospectively ECG-gated multislice spiral CT. *Circulation* 2000; 102:2823–2828
- Kuettner A, Beck T, Drosch T, et al. Diagnostic accuracy of noninvasive coronary imaging using 16-detector slice spiral computed tomography with 188 ms temporal resolution. *J Am Coll Cardiol* 2005; 45:123–127
- Mollet NR, Cademartiri F, Krestin GP, et al. Improved diagnostic accuracy with 16-row multislice computed tomography coronary angiography. *J Am Coll Cardiol* 2005; 45:128–132
- Hunold P, Vogt FM, Schermund A, et al. Radiation exposure during cardiac CT: effective doses at multi-detector row CT and electron beam CT. *Radiology* 2004; 226:145–152
- Cline H, Coulam C, Yavuz M, et al. Coronary artery angiography using multislice computed tomography images. *Circulation* 2000; 102:1589–1590
- Becker C, Schatzl M, Feist H, et al. Assessment of the effective dose for routine protocols in conventional CT, electron beam CT and coronary angiography. *Rofo Fortschr Geb Rontgenstr Neuen Bildgeb Verfahr* 1999; 170:99–104
- Kalra MK, Maher MM, Toth TL, et al. Strategies for CT radiation dose optimization. *Radiology* 2004; 230:619–628
- Morin RL, Gerber TC, McCollough CH. Radiation dose in computed tomography of the heart. *Circulation* 2003; 107:917–922
- Nickoloff EL, Alderson PO. Radiation exposures to patients from CT: reality, public perception, and policy. *AJR* 2001; 177:285–287
- Becker C, Schatzl M, Feist H, et al. Assessment of the effective dose for routine protocols in conventional CT, electron beam CT and coronary angiography. *Rofo Fortschr Geb Rontgenstr Neuen Bildgeb Verfahr* 1999; 170:99–104
- Bae KT, Hong C, Whiting BR. Radiation dose in multidetector row computed tomography cardiac imaging. *J Magn Reson Imaging* 2004; 19:859–863
- Flohr TG, Schoepf UJ, Kuettner A, et al. Advances in cardiac imaging with 16-section CT systems. *Acad Radiol* 2003; 10:386–401
- Nieman K, Oudkerk M, Rensing BJ, et al. Coronary angiography with multi-slice computed tomography. *Lancet* 2001; 357:599–603
- Coles DR, Smail MA, Wilde P, et al. Comparison of radiation doses from multislice computed tomography coronary angiography and conventional diagnostic angiography. *J Am Coll Cardiol* 2006; 47:1840–1845

24. Brenner DJ, Elliston CD, Hall EJ, et al. Estimated risks of radiation-induced fatal cancer from pediatric CT. *AJR* 2001; 176:289–296
25. Yoshizumi TT, Goodman PC, Frush DP, et al. Validation of MOSFET technology in CT organ dose assessment: MOSFET vs TLD. *AJR* 2007; 188:1332–1336
26. Yoshizumi T, Sarder M, Goodman P, Frush D, Barnes L, Nguyen G. Application of MOSFET technology in CT organ dose assessment. *Med Phys* 2003; 30:1422
27. Toncheva G, Nguyen G, Barnes L, Frush DP, Samei E, Yoshizumi T. Physics characterization of μ -MOSFET detectors for use in CT dosimetry. *Med Phys* 2004; 31:1850
28. Kruger RL, McCollough CH, Zink FE. Measurement of half-layer in x-ray CT: a comparison of two noninvasive techniques. *Med Phys* 2000; 27:1915–1919
29. DeMarco JJ, Cagnon CH, Cody DD, et al. A Monte Carlo based method to estimate radiation dose from multidetector CT (MDCT): cylindrical and anthropomorphic phantoms. *Phys Ed Biol* 2005; 50:3989–4004
30. Radtke WA. Vascular access and management of its complications. *Pediatr Cardiol* 2005; 26:140–146
31. Waldman JD, Swenson RE. Therapeutic cardiac catheterization in children. *West J Med* 1990; 153:288–295
32. Hurwitz LM, Yoshizumi TT, Reiman RE, et al. Radiation exposure to the fetus from body MDCT during early gestation. *AJR* 2006; 186:871–876
33. Jaffe T, Nelson R, Johnson GA, et al. Optimization of multiplanar reformations from isotopic data sets acquired on a 16-slice multidetector helical CT scanner. *Radiology* 2006; 238:292–299
34. Hurwitz L, Yoshizumi T, Reiman R, et al. Radiation dose to the female breast from 16-MDCT body imaging protocols. *AJR* 2006; 186:1718–1722
35. Frush DF, Yoshizumi T. Conventional and CT angiography in children: dosimetry and dose comparisons. *Pediatr Radiol* 2006; 36[suppl 14]:154–158
36. Brenner DJ. Is it time to retire the CTDI for CT quality assurance and dose optimization? *Med Phys* 2005; 32:3225–3226
37. Slovis TL. Children, computed tomography radiation dose, and the as low as reasonably achievable (ALARA) concept. *Pediatrics* 2003; 112:971–972
38. Soubra M, Cygler J, Mackay GF. Evaluation of a dual bias dual metal-oxide-silicon semiconductor field effect transistor detector as a radiation dosimeter. *Med Phys* 1994; 21:567–572
39. International Commission on Radiation Protection. *Recommendation of the International Commission on Radiological Protection. ICRP 60*. Oxford, England: Pergamon, 1991
40. Cristy M. Active bone marrow distribution as a function of age in humans. *Phys Med Biol* 1981; 26:389–400
41. Shrimpton PC, Wall BF. Reference doses for paediatric computed tomography: radiation protection. *Dosimetry* 2000; 90:249–252
42. Huda W, Scalzetti EM, Levin G. Technique factors and image quality as functions of patient weight at abdominal CT. *Radiology* 2000; 217:430–435
43. Siegel MJ. Radiation dose and image quality in pediatric CT: effect of technical factors and phantom size and shape. *Radiology* 2004; 233:515–522
44. Gajewski KK. Cardiology. In: Robertson J, Shilkofski N, eds. *The Harriet Lane handbook*, 17th ed. Philadelphia, PA: Mosby, 2005:164–165
45. ICRP 1991 Recommendations of the International Commission on Radiological Protection ICRP publication 60. *Ann ICRP* 1991; 21:79–89
46. McCollough CM, Schueler BA. Calculation of effective dose. *Med Phys* 2000; 27:828–837
47. Greil GF, Schoebinger M, Kuettner A, et al. Imaging of aortopulmonary collateral arteries with high-resolution multidetector CT. *Pediatr Radiol* 2006; 36:502–509
48. Goo HW, Suh DS. Tube current reduction in pediatric non-ECG-gated heart CT by combined tube current modulation. *Pediatr Radiol* 2006; 36:344–351
49. Donnelly LF, Emery KA, Brody AS, et al. Minimizing radiation dose for pediatric body applications of single-detector helical CT: strategies at a large children's hospital. *AJR* 2001; 176:303–306
50. Paterson A, Frush DP, Donnelly LF. Helical CT of the body: are the settings adjusted for pediatric patients? *AJR* 2001; 176:297–301
51. Committee on the Biological Effects of Ionizing Radiation (BEIR V), National Research Council. *Health effects of exposure to low levels of ionizing radiation: BEIR V*. Washington, DC: National Academies Press, 1990
52. Pierce DA, Preston DL. Radiation-related cancer risks at low doses among atomic bomb survivors. *Radiat Res* 2000; 152:178–186
53. Pierce DA, Shimizu Y, Preston DL, et al. Studies of mortality of atomic bomb survivors. Report 12, part 1. Cancer: 1950–1990. *Radiat Res* 2000; 146:1–27
54. Huda W, Scalzetti EM, Roskopf M. Effective doses to patients undergoing thoracic computed tomography examinations. *Med Phys* 2000; 27:838–844
55. Pages J, Buls N, Osteaux M. CT doses in children: a multicentre study. *Br J Radiol* 2003; 76:803–811
56. Flanigan DP, Keifer TJ, Schuler JJ, et al. Experience with iatrogenic pediatric vascular injuries: incidence, etiology, management, and results. *Ann Surg* 1983; 198:430–442
57. Bacher K, Bogaert E, Lapere R, et al. Patient-specific dose and radiation risk estimation in pediatric cardiac catheterization. *Circulation* 2005; 111:83–89
58. Rassow J, Schmaltz AA, Hentrich F, et al. Effective doses to patients from paediatric cardiac catheterization. *Br J Radiol* 2000; 73:172–183
59. Lin PH, Dodson TF, Bush RL, et al. Surgical intervention for complications caused by femoral artery catheterization in pediatric patients. *J Vasc Surg* 2001; 34:1071–1078
60. Taylor LM Jr, Troutman R, Feliciano P, et al. Late complications after femoral artery catheterization in children less than five years of age. *J Vasc Surg* 1990; 11:297–306
61. Smith C, Green RM. Pediatric vascular injuries. *Surgery* 1981; 90:20–31
62. Leblanc J, Wood AE, O'Shea MA, et al. Peripheral arterial trauma in children: a fifteen year review. *J Cardiovasc Surg* 1985; 26:325–331
63. Frush DP, Herlong JR. Pediatric thoracic CT angiography. *Pediatr Radiol* 2005; 35:11–25
64. Balter S. Radiation safety in the cardiac catheterization laboratory: operational radiation safety. *Catheter Cardiovasc Interv* 1999; 47:347–353
65. Johnson LW, Moore RJ, Balter S. Review of radiation safety in the cardiac catheterization laboratory. *Cathet Cardiovasc Diagn* 1992; 25:186–194
66. Hall EJ. From chimney sweeps to astronauts: cancer risks in the work place—the 1998 Lauriston Taylor lecture. *Health Phys* 1998; 75:357–366